Dissociative Electron Transfer in Donor−Peptide−Acceptor Systems: Results for Kinetic Parameters from a Density Functional/Polarizable Continuum Model

Vincenzo Barone,[†] Marshall D. Newton,[‡] and Roberto Improta*[,†,§]

Dipartimento di Chimica, Università Federico II, Complesso Monte S. Angelo, via Cintia, I-80126 Napoli, Italy, Brookhaven National Laboratory, Upton, New York 11973-5000, and Istituto di Biostrutture e Bioimmagini, CNR, via Mezzocannone 16, 80134 Napoli, Italy

Received: October 11, 2005; In Final Form: April 27, 2006

The main structural and electronic factors playing a role in intramolecular dissociative electron transfer of a simple donor−peptide−acceptor (D−peptide−A) model have been investigated by an integrated computational protocol based on the density functional theory, its time-dependent extension, and the polarizable continuum model. Our results allow us to elucidate the electronic states involved in the process and how they are perturbed by the orientation of the donor and the acceptor with respect to the peptide chain and by the presence of the solvent. We also report a semiquantitative estimation of the rate constant governing electron transfer obtained by a direct quantum mechanical evaluation of all the terms entering the kinetic expressions based on the Marcus theory and its extensions.

1. Introduction

Understanding and predicting the role of different structural and electronic factors in tuning the rate of electron transfer (ET) has, at least, a twofold interest. On one hand, better control of the reactivity is very important for photolysis, thermolysis, and radical reactions of biological and technological interest.[1−4] On the other hand, a deeper understanding of the intrinsic and environmental effects tuning ET rates will have a significant impact in emerging applications such as sensors and biosensors[2] or molecular electronic devices.[3]

Like nondissociative ETs, intramolecular dissociative electron transfer (DET) processes are tuned by the relative orientation of the exchanging orbitals, the distance between the donor (D) and acceptor (A) redox centers, and the nature of the molecular bridge. However, despite the relevance of DET in several processes of biological and/or technological interest, systematic computational studies in this area are just beginning. This prompted us to start a comprehensive research program on DET involving suitable spacers, exploiting the availability of new computational approaches rooted in the density functional theory (DFT), its time-dependent extension (TD-DFT), and the so-called polarizable continuum model (PCM) for describing solvent effects.

Because the peptide chains are essential in assisting long-range ET in proteins,[2] several research groups have analyzed well-defined D−peptide−A models, including proline,[5] α amino isobutyric acid (Aib),[6] and other amino acid residues.[7] Following this approach, the systems examined in the present study (see Figure 1) involve a phthalimide (Pht) donor, a peroxo (Per) acceptor and a bridge formed by Aib residues. The intramolecular ET reaction in these compounds is a concerted dissociative process strongly influenced by the large inner reorganization associated with elongation of the cleaving O_1-O_2 bond.[8] The reduction of the peroxide is thus irreversible and kinetically very slow.[9] Because of this ET sluggishness, the electron is first injected by the electrode onto the phthalimide end of the peptide, leading to the corresponding radical anion. The reaction is kinetically fast because only solvent reorganization and negligible inner reorganization are involved in the heterogeneous process. As a consequence, the rate-determining step is the subsequent intramolecular transfer of the electron to the peroxide end of the peptide. While the general process is characterized quite well from an experimental point of view, the role of different structural and electronic factors in tuning the DET efficiency is still not fully understood. In a previous conformational study of the initial radical anion,[6] we showed that three different orientations of the donor with respect to the peptide bridge are possible. The two most relevant conformations can be labeled as Φ_{hel} ($\phi_0 \approx -60°$, $\psi_0 \approx -40°$) and Φ_{pII} ($\phi_0 \approx -60°$, $\psi_0 \approx \pm 180°$). The most stable conformation for the peptide chain is the 3_{10}-helix, but, for $n = 3$, the α-helix structure corresponds to a local minimum for the anion compound (the initial state involved in the DET process), which is only ∼3 kcal/mol less stable than the 3_{10}-helix.

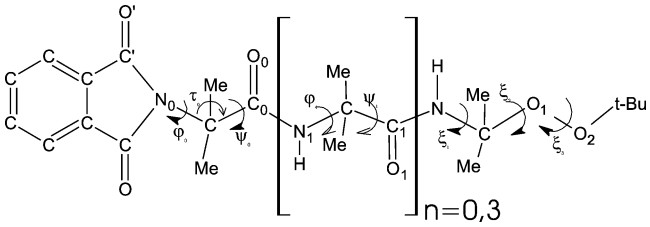

Figure 1. Schematic drawing and atom labeling of the system under study.

On the basis of the previous analysis, in the present paper we tackle the study of the mechanism and the dynamics of the DET process in the radical anion of Aib0, that is, the compound in which the spacer between the donor and the acceptor is constituted by a single peptide bond, while the effect of the bridge lengthening will be examined in a forthcoming study. In particular, we will try to answer the following questions:

* Corresponding author. E-mail: robimp@unina.it; phone: +39 081 674208; fax: +39 081 674090.
† Università Federico II.
‡ Brookhaven National Laboratory.
§ Istituto di Biostrutture e Bioimmagini.

10.1021/jp0557969 CCC: $33.50
Published on Web 06/02/2006

TABLE 1: Comparison between the Computed Values (6-31G(d) Basis Set) of the Main Kinetic Parameters for the DET Process and the Experimental Results[a]

conformation	$\Delta G^{\ddagger}$	bond elong. at the TS	H_{DA}	λ	log K_{DET}[b] eq 1	log K_{DET}[b] eq 2
Aib0$_{t-but}$[c] Φ_{hel}	0.512 (0.460)	0.280	0.065 (0.119)	1.00	4.20 (5.61)	4.33
water solution[c]	0.564 (0.548)	0.278	0.038 (0.0625)	1.00	2.86 (3.56)	2.98
gas-phase geometry optimization + PCM gas phase	0.512 (0.460)	0.270	0.129 (0.081)	1.00	4.80 (5.27)	4.91
	0.522 (0.501)	0.295	0.118 (0.101)	1.00	4.55 (4.77)	4.69
Φ_{pII}	0.654 (0.616)	0.260	0.127 (0.158)	1.32	2.38 (3.21)	2.52

[a] $\Delta G^{\ddagger}$, H_{DA}, and λ values are given in electronvolts (eV). Bond elongation at the TS is given in angstroms (Å). The results obtained by using the 6-31+G(d,p) basis set are given in parentheses. [b] Experimental result (relative to AibO$_{t-but}$): 4.70.[27] [c] From ref 13.

1. What are the electronic states relevant to the DET process? Does a sequential hopping mechanism play any role?
2. What are the active modes promoting the DET?
3. What is the influence of the orientations of the donor and the acceptor with respect to the peptide chain?

Besides the intrinsic interest of gaining a deeper insight into the fundamental microscopic chemicophysical effects that modulate ET, this study allows us to explore the potentiality of integrating accurate quantum mechanical computations in the condensed phase with well-assessed theoretical models to study the ET process. The cornerstone of most recent computational approaches[10] to ET modeling is surely the Marcus equation,[14]

$$K_{ET} = \frac{2\pi}{\hbar}\frac{{H_{DA}}^2}{\sqrt{4\pi\lambda k_B T}}\left[\exp\left(-\frac{\Delta G^{\ddagger}}{k_B T}\right)\right] \quad (1)$$

whose basic ingredients are the electronic coupling between the donor and the acceptor mediated by the bridge (H_{DA}), the reorganization energy (λ), and the activation free energy ($\Delta G^{\ddagger}$). The above expression is valid for the for thermal ET within the nonadiabatic regime (i.e., weak coupling between the donor and the acceptor) in the case of harmonic nuclear motion (high temperature). It can easily be extended to treat optical ET and has been successfully applied to the study of many thermal and optical reactive processes.[10] With the increasing attention paid to DET,[11,12] extensions of eq 1 have been developed, in which the contribution of the bond dissociation energy (BDE) of the scissile bond to the reorganization energy is explicitly considered:

$$K_{DET} = \frac{2\pi}{\hbar}\frac{{H_{DA}}^2}{\sqrt{16\pi k_B T \Delta G_0^{\ddagger}\exp(-2\beta\Delta r)}}\left[\exp\left(-\frac{\Delta G^{\ddagger}}{k_B T}\right)\right] \quad (2)$$

In eq 2, $\Delta G_0^{\ddagger} = (\mathrm{BDE} + \lambda)/4$, Δr is the bond elongation at the transition state (TS), and β represents the curvature of the Morse function that can approximate the potential energy curve associated with the breaking bond.[11b] Here we will show that all the terms of the above equations can be computed in the framework of a TD-DFT/PCM approach,[13] leading to semiquantitative agreement with experimental rates and underscoring some limits of standard models.

2. Computational Details

All the computations were performed using a development version of the Gaussian package,[15] the PBE0 hybrid functional,[16] and standard 6-31G(d) and 6-31+G(d,p) basis sets.[17] For the TD-DFT calculations, we used the PBE0 hybrid functional, which, despite the absence of adjustable parameters, has been shown to provide excitation spectra in very good agreement with experimental results and usually better than those obtained by other hybrid functionals.[18] Test calculations on 1-methylphthalimide show that this functional is able to correctly reproduce the excitation spectra of this compound. For example, PCM/TD-PBE0/6-31+G(d,p)//PCM/PBE0-6-31G(d) calculations in acetonitrile predict the presence of two strong absorption peaks at 5.45 and at 5.88 eV with oscillator strengths of 0.25 and 0.66, respectively. The computed spectrum is thus very close to the experimental one, which exhibits a strong absorption band at ∼5.7 eV, with an additional and less intense peak at ∼5.25 eV.[19] PBE0 calculations have also successfully been applied in studies of Pht−Aib−Per systems. For example, the calculated variation of the adiabatic electron affinities (EA) with the number of Aib units is in good agreement with the observed electrochemical behavior. Furthermore, it provides a good energetic description of the peroxo O−O bond breaking (vide infra and ref 13). Bulk solvent effects in dimethylformamide (DMF) solution were taken into account by the latest implementation[20] of the PCM (dielectric constant for DMF = 37.8).[21] The reliability of this computational protocol for the study of radical species in condensed phases is well documented.[22] Excited-state calculations have been performed by the same basis sets and functional using the TD-DFT approach, including nonequilibrium solvent effects.[23] If not otherwise stated, in all of the systems studied, the phthalimide moiety adopts a Φ_{hel} orientation with respect to the peptide chain. The calculation of the DET rate constant was performed according to eqs 1 and 2 by using the theoretical methodology presented in ref 13. In particular, the activation free energy is directly given by the analysis of the potential energy surfaces (PES) associated with the DET performed in DMF solution at the PCM-PBE0 and PCM-TD-PBE0 levels, that is, taking into account solvent effects by the PCM. We recall in this connection that PCM results have the status of free energies. The analysis of PES also provides the value of BDE and Δr necessary to implement eq 2. For β, we used the value of 2.8, estimated by Maran et al. on the basis of the average vibrational O−O stretching frequency of peroxides.[11]

Next, the electronic coupling H_{DA} is computed from the energy difference between the adiabatic states at the TS by using the generalized Mulliken−Hush model.[24] Finally, the solvent reorganization energy (λ) is estimated in terms of the difference between the equilibrium and nonequilibrium solvation energies for the A^- state.[13] This procedure has provided rate constants for Aib0 and for its longer analogue Aib1 (containing one additional Aib unit in the bridge) in good agreement with the experimental results. Furthermore, the estimated values for $\Delta G^{\ddagger}$, H_{DA}, and λ are reasonable and similar to the those obtained from experiments or from other theoretical approaches (see Table 1).[13]

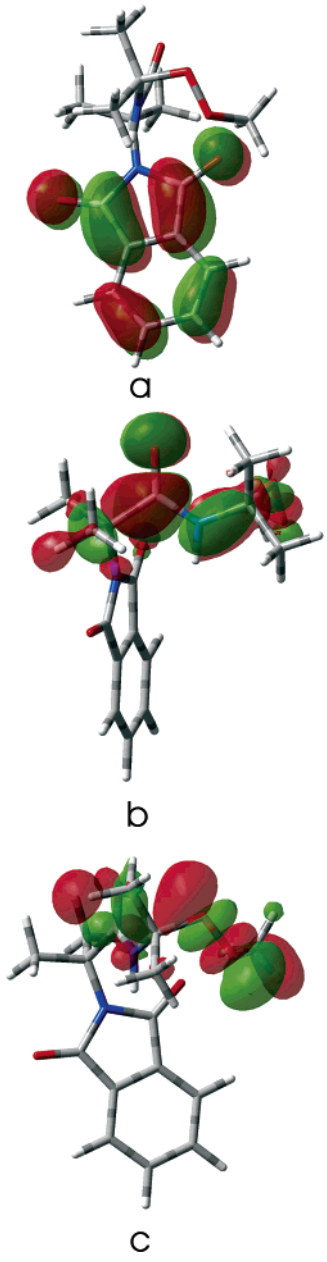

Figure 2. Schematic drawing of the molecular orbitals potentially relevant for the DET process: (a) SOMO of Aib0 (bearing the unpaired electron in the D^- state); (b) π^* orbital of the peptide unit of Aib0 (bearing the unpaired electron in the B^- state); and (c) σ^* orbital of the peroxo moiety (bearing the unpaired electron in the A^- state).

3. Results

As a preliminary step, it is worthwhile to ascertain which electronic states and molecular orbitals (see Figure 2) are potentially relevant to the DET process.

As mentioned above, electron injection in Aib0 leads to the formation of an anion localized on the phthalimide ring that will act as a donor in the subsequent DET process. In the resulting electronic state (hereafter referred to as D^-), the electron is almost entirely localized in the molecular orbital depicted in Figure 2a, that is, the lowest unoccupied molecular orbital (LUMO) of the neutral Aib0 (and of a neutral phthalimide ring) and becomes the singly occupied molecular orbital (SOMO) of D^-. The rate-determining step of the DET process consists of the transfer of an electron from the phthalimide ring to the peroxo moiety, producing the A^- state, in which the electron is localized in the peroxo σ^* orbital (see Figure 2c). After a small lengthening of the O_1-O_2 bond length relative to equilibrium, this orbital is the LUMO of Aib0 up to the TS. In a sequential hopping mechanism, a state in which the electron is localized on the bridge (B^- state) would be involved. In our case, it would be localized mainly on the π^* orbital of the Aib unit (see Figure 2b). D^-, A^-, and B^- are the lowest energy states of Aib0 up to the TS. There is another electronic state of comparable energy (~1.6 eV less stable than D^-), in which the electron is localized in a higher energy π^* orbital of the phthalimide ring (see Figure S1 in the Supporting Information). However, since the energy of this state is not influenced by the O_1-O_2 bond lengthening and the associated PES is almost "parallel" to that of D^-, this state should not be involved in the DET process.

3.1. Adiabatic Energy Curve for the DET. As a first step of our analysis, we studied the energy of the *adiabatic* states most relevant for the DET as a function of the O−O bond stretching in the peroxo moiety (see Figures 3 and 4) by performing ground-state geometry optimizations in DMF solution for different values of the O_1-O_2 bond length, followed by TD/PBE0 calculations to obtain excited-state energies.

Within the Marcus theory for weakly coupled D and A groups, the energy is expressed as a function of the solvent nonequilibrium polarization. Therefore, besides the O_1-O_2 bond distance, we should also include a generalized solvent coordinate. However, as a first approximation, we focus on the scissile bond coordinate only, treating the solvent coordinate on the same footing as the remaining intramolecular degrees of freedom. In all the plots shown in Figures 3, 4, 7, and 8, the solvent is thus fully equilibrated on the ground-state electron density for each O_1-O_2 bond distance, while, for the excited states, solvation effects are included at the nonequilibrium level (thus giving access to vertical energy gaps). Several considerations suggest that this assumption should not be critical, at least concerning the main conclusions of our study. As discussed below, the bond elongation at the TS and the $\Delta G^{\ddagger}$ values provided by our procedure are indeed in good agreement with those estimated on the basis of the experimental results. Furthermore, our calculations indicate that equilibrium solvation energy is almost constant until the proximity of the TS. In the TS region, it reaches a shallow minimum (~0.07 eV), while, after ET occurs, it starts increasing since solvent favors the A^- state, where the negative charge is localized on the small peroxo moiety. Thus, in our case, solvent does not strongly affect the location and the stability of the TS (see also Section 3.3).

The O_1-O_2 stretching is not significantly coupled to other geometrical parameters up to a bond distance of ~1.7 Å, that is, close to the TS for the ET process. In fact, for an O_1-O_2 bond length of 1.68 Å, a fully relaxed geometry optimization decreases the energy by only 0.05 eV with respect to a single-point calculation in which all the remaining geometric parameters are frozen at their values in the absolute energy minimum of the D^- state.

Our calculations thus indicate that, as already suggested for the DET in similar peroxo compounds,[26] the role played by vibrational degrees of freedom other than the O_1-O_2 bond stretching is not of major significance. The geometrical parameters of the bulky aromatic phthalimide group are not strongly influenced by the presence of an extra electron, aside from a small lengthening (~0.03 Å) of the carbonyl CO bonds. This implies that, in our system, vibrational reorganization effects are not very important. As a consequence, even though in principle the role of Franck−Condon factors on the DET rate

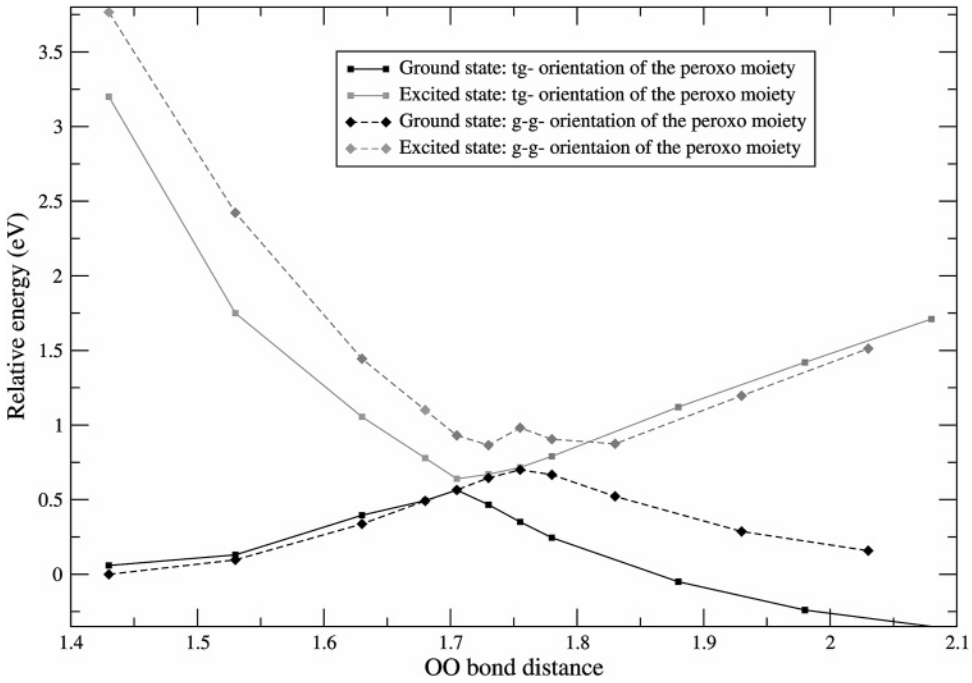

Figure 3. Energy (relative to the D^- absolute minimum) of the ground and excited electronic states of Φ_{hel}Aib0, obtained by TD-PBE0/6-31G-(d)//PBEO/6-31G(d) calculations as a function of the O_1-O_2 bond distance for different orientations of the peroxo moiety with respect to the peptide bridge.

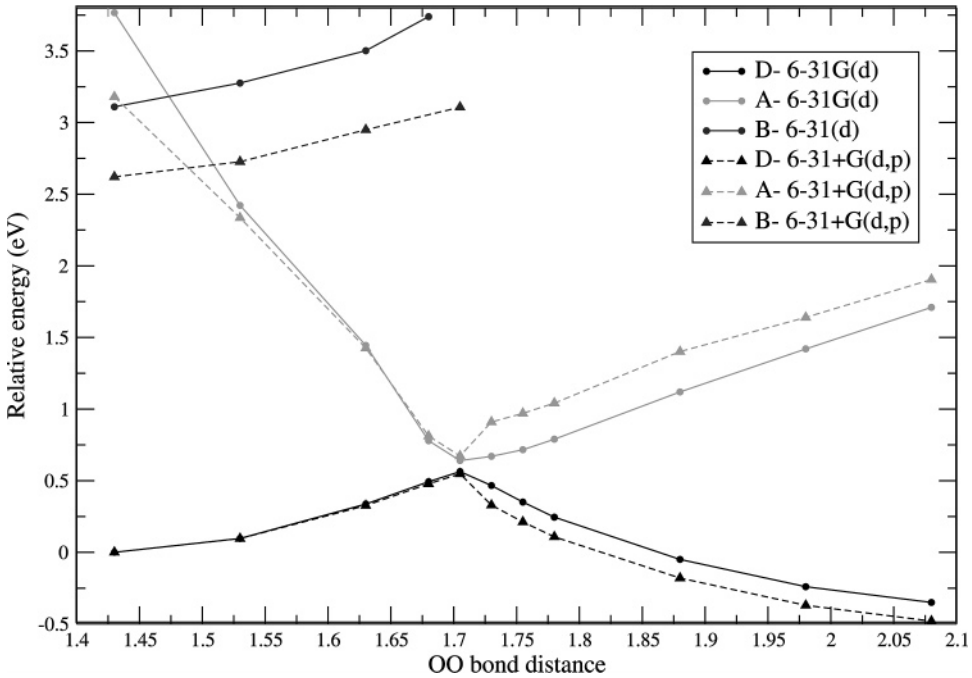

Figure 4. Energy (relative to the D^- absolute minimum) of the most relevant states of the Aib0 system, obtained by TD-PBE0//PBEO/6-31G(d) calculations. The green lines refer to the B^- state. The black and the red lines refer to the D^- and A^- states, respectively, before and after the TS (the states are switched after the TS). The results refer to the most stable conformer for the ground electronic state (i.e., g^-g^- up to 1.68 Å and the tg^- conformer thereafter).

should be considered, as a first approximation, we did not take it into account.

Up to an O_1-O_2 bond distance of ∼1.68 Å, the ground adiabatic state coincides with the D^- state. For longer bond distances, the ET process starts, and the σ^* orbital of the peroxo moiety begins to contribute to the SOMO of the Aib0 ground state. This process is assisted by a certain geometric rearrangement of the peroxo moiety, mainly consisting of the shortening of the C−O bond lengths, as reflected by the fact that the SOMO takes on some C−O bonding character (see Figure 2), and also by the relaxation of the phthalimide geometry toward that of the neutral ring. The ET process can be "assisted" by a rearrangement of the dihedral angles of the peroxo moiety. In particular, ξ_1 (ξ_2 is always approximately −60°) shifts from its equilibrium value of approximately −60° (g^-g^- conformer) to a trans conformation, $\xi_1 \approx 180°$ (tg^- conformer), allowing the formation of an interaction between the last NH group and the peroxo moiety that stabilizes the presence of a negative charge on the peroxo moiety (see Figure 5). The maximization of this interaction is likely the cause of small bond-angle shifts of the

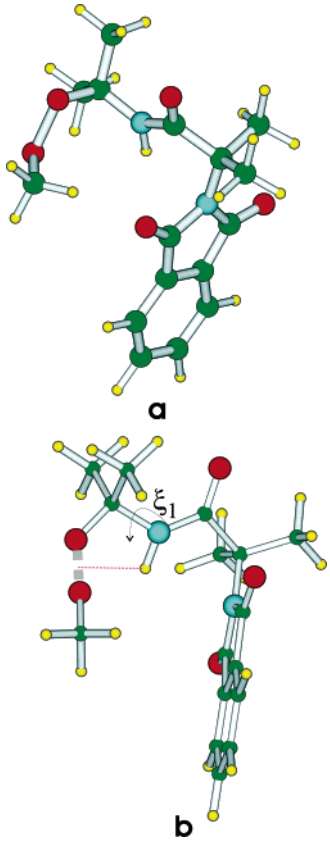

Figure 5. Schematic drawing of the g^-g^- (a) and tg^- (b) conformers of ϕ_{hel}Aib0.

backbone, leading to a decrease in the N−H•O_2 distance. Inspection of Figure 3 shows that, for the D^- state, the g^-g^- conformer is more stable than tg^-, but, when approaching the TS (where a partial negative charge starts developing on the peroxo moiety because of the highest occupied molecular orbital (HOMO)−LUMO mixing), the two conformers become almost isoenergetic. The tg^- conformer is always the most stable one for the A^- state. According to our computations, the presence of multiple conformers for the peroxo moiety could have a significant influence on the dynamics of the DET process: when the peroxo moiety is constrained in the g^-g^- conformation, the activation energy for the ET process increases by ∼0.15 eV, and the O_1-O_2 distance at the TS increases by ∼0.05 Å. Beyond the TS, the unpaired electron is localized on the peroxo moiety, with the ground electronic state corresponding to the A^- state and the first excited electronic state corresponding to the D^- state.

At the TS, the O−O bond length is 1.71 Å. Since the equilibrium value is ∼1.44 Å, the computed bond lengthening is 0.27 Å, in good agreement with the estimate of 0.241 Å based on the German/Kutznetov theory.[12] Furthermore, the computed activation free energy of 0.564 eV (0.542 eV at the 6-31+G-(d,p) level) is in good agreement with the value of ∼0.6 eV obtained from an analysis of the experimental data for similar compounds.[25]

The B^- state is always significantly less stable than the A^- state (by ∼3 eV in the region of TS), and its energy relative to the ground state has a negligible dependence on the O_1-O_2 bond length. Only in the vicinity of the equilibrium geometry of the D^- state is B^- more stable than A^-. However, this region of the PES should not be significant for the thermal DET process, but would be for photoexcited ET. In this latter case, a conical intersection between the B^- and the A^- states should be expected

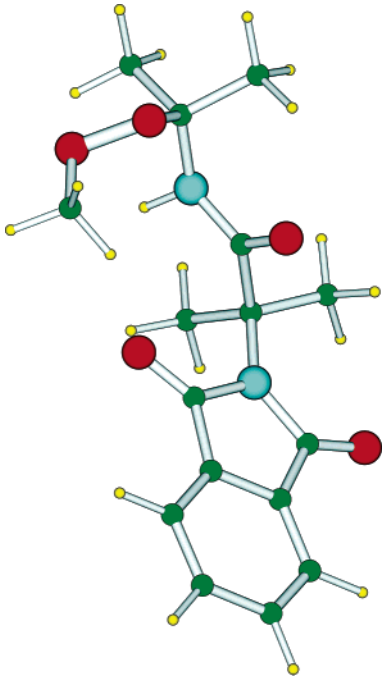

Figure 6. Schematic drawing of the g^-g^-conformer of Φ_{pII}Aib0.

immediately after the Franck−Condon region. For O_1-O_2 bond lengths beyond the TS value, the B^- state is always at least 3 eV less stable than A^- and D^- and is not involved in the six lowest energy transitions.

Use of a more extended basis set does not significantly change the qualitative conclusions of our analysis. From a quantitative point of view, the A^- and (especially) B^- states are stabilized with respect D^-, whereas the computed activation energy and bond lengthening at the TS are similar to those obtained at the 6-31G(d) level.

3.2. Influence of the Orientation of the Donor with Respect to the Peptide Chain. To verify the effect of the orientation of the donor on the DET, we repeated the most important steps of the above analysis for Φ_{pII}Aib0 (see Figure 6).

In this case, the tg^- conformer is quite close in energy to its g^-g^- counterpart, and, for O_1-O_2 bond distances greater than 1.60 Å, it indeed becomes the most stable conformer. The energies of the relevant electronic states of the tg^- conformer as a function of the O_1-O_2 distance are shown in Figure 7. The behavior of the lowest energy excited states is similar to that described above for Φ_{hel}, and this is also the case for the predicted activation energy and O−O bond elongation at the TS. On the other hand, the energy gap at the TS (determining the electronic coupling) is larger than that for Φ_{hel}, and the PES associated with the first excited state exhibits a "spike" after the TS. This feature is likely due to the different behavior of the ξ_2 dihedral of the peroxo moiety. As already mentioned for ξ_1, ξ_2 also shifts from a g^- ($\approx -60°$) to an eclipsed conformation during DET. The much lower stability of this conformation for the D^- state is at the root of the larger energy gap predicted by TD-PBE0 calculations.

3.3. Influence of the Solvent on the PES. Figure 8 shows the gas-phase energies of the adiabatic A^- and D^- states as a function of the O_1-O_2 bond length for Φ_{hel}Aib0.

Although the predicted activation energy is in good agreement with that computed in DMF solution, the curve associated with the excited state is much less regular, and the curves associated with the ground and excited states run almost parallel between 1.7 and 1.9 Å. A polar solvent helps to stabilize a negative

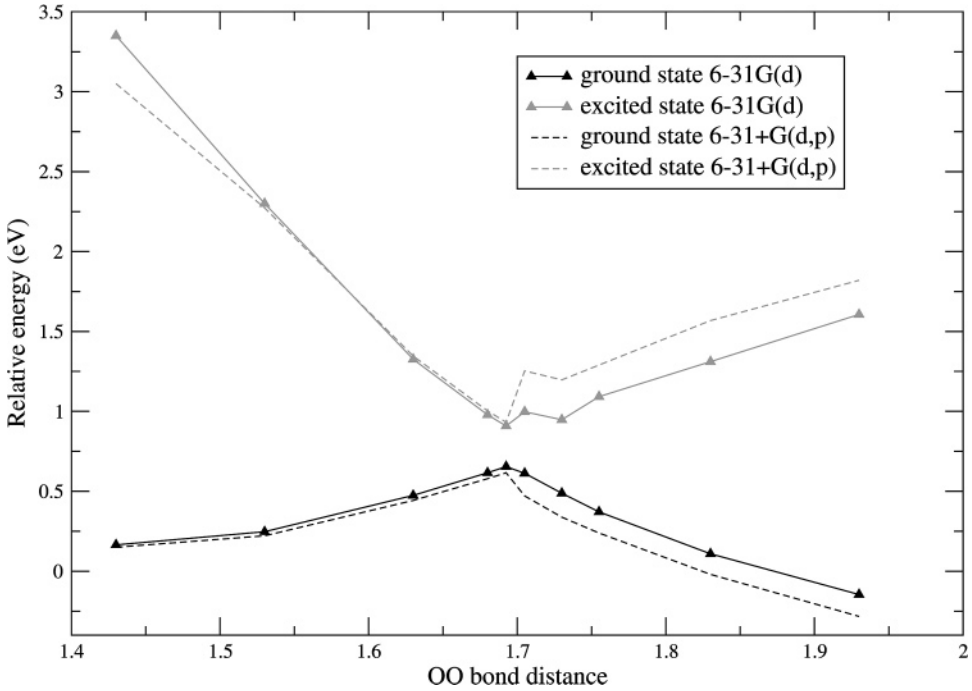

Figure 7. Energy (relative to the D^- absolute minimum) of the most relevant states of the Φ_{pII}Aib0 system, obtained by TD-PBE0/6-31G(d)//PBEO/6-31G(d) calculations as a function of the O_1-O_2 bond distance for the tg^- orientation of the peroxo moiety with respect to the peptide bridge.

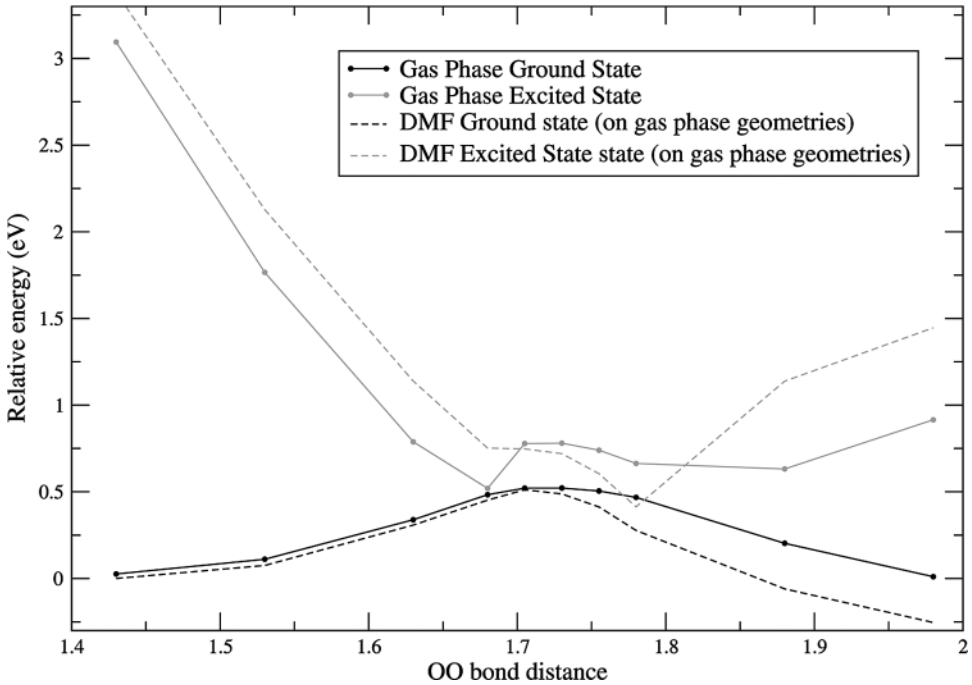

Figure 8. Energy (relative to the D^- absolute minimum) of the ground and excited electronic states of Φ_{hel}Aib0, obtained by TD-PBE0/6-31G-(d)//PBEO/6-31G(d) calculations as a function of the O_1-O_2 bond distance in the gas phase. Dashed lines refer to the DMF correction obtained by single-point PCM calculations using the gas-phase optimized geometries.

charge on the peroxo moiety (much smaller than the phthalimide ring), whereas, in the gas phase, the phthalimide ring orbitals significantly contribute to the SOMO in a larger region of the PES (up to an O_1-O_2 bond length of $\sim$1.85 Å).

Inspection of the gas-phase optimized geometries shows that the persistence of a partial negative charge on the phthalimide ring after the TS leads also to the overstabilization of the nonconventional hydrogen bond between the NH group and the phthalimide ring (see Figure 5). In DMF solution, this interaction becomes weaker, and thus the NH group can smoothly shift from interacting with the phthalimide ring to interacting with the peroxo group, thus assisting the DET process. In the gas phase, the NH group is indeed directed toward the phthalimide ring, and the NH$\cdots$O$_2$ distance is always longer than that in DMF until the ET process is completed ($O_1-O_2 \approx 1.88$ Å). In a wide region of the PES around the TS, the geometries optimized in vacuo and in DMF solution are significantly different. As a consequence, also taking into account solvent effects by PCM single-point calculations on the gas-phase optimized geometries (dashed lines of Figure 8) does not restore a satisfactory agreement with the results obtained by using geometries optimized in DMF solution.

Another remarkable difference between the PES computed in vacuo and that computed in DMF is that the energy decrease of the adiabatic states associated with A^- is significantly softer in the former case, suggesting that, in agreement with chemical intuition, the DET process is thermodynamically favored by a polar solvent.

3.4. Calculation of the Rate Constant for DET. In the final step of our analysis, we evaluated how the effects discussed in the above sections influence the DET rate constant. For each system, the appropriate calculated values for $\Delta G^{\ddagger}$ and H_{DA} were inserted in eq 1. For λ, we employed the value computed for Φ_{hel} (O−O bond distance of 1.53 Å). It is noteworthy that our result (1.0 eV) is not far from the estimate of 0.9 eV obtained by Donkers et al.[26] using an empirical equation and a number of simplifying approximations (e.g., spherical donor and acceptor with equal solvation energies). Interestingly, application of eq 2 provides results very similar to those obtained by using the simpler approximation represented by eq 1, thus supporting the reliability of our conclusions.

As previously shown,[13] for Φ_{hel}, our procedure provides a DET rate at room temperature ($10^{3.5}$) about an order of magnitude smaller than the experimental value ($10^{4.7}$). This result can be considered quite satisfactory taking into account the lack of any adjustable parameter in our computational approach and the replacement of the experimental *tert*-butyl group by a methyl group, which, according to our calculations,[13] leads to a decrease in the DET rate constant.

The agreement with the experimental rate constant decreases appreciably when using the results from gas-phase geometry optimizations. In fact, the computed value based on the terminal methyl group happens to be close to the experimental one, (involving a terminal *t*-butyl group), suggesting that, if the terminal methyl group were replaced by a *t*-butyl group, the computed rate constant would be overestimated by ∼2 orders of magnitude with respect to the experimental one.

It is instead noteworthy that the computed DET rate for Φ_{pII} is of the right order of magnitude, though underestimated with respect to that obtained for Φ_{hel}.

4. Concluding Remarks

The present paper is devoted to a detailed analysis of the different physicochemical factors playing a role in tuning DET in a phthalimide−Aib−peroxide model. From a quantitative point of view, the combined use of methods rooted in the density functional approach, its time-dependent extension, and continuum solvent models, allows us to obtain results in fair agreement with experiment concerning structural and kinetic aspects. On these grounds, it is possible to point out a number of key issues for a deeper interpretation of experimental results:

1. The PES for the DET cannot be strictly considered one-dimensional, since the rearrangement of the dihedral angle of the peroxo moiety is coupled to the O−O stretching. The extent of this rearrangement depends on the orientation of the phthalimide ring, involving only ξ_1 for Φ_{hel} and both ξ_1 and ξ_2 for Φ_{pII}.

2. Since, in the region of the PES close to the TS, the B^- state is much less stable than A^- and D^- (by at least by 3 eV), a sequential hopping mechanism should not play any role in the DET.

3. The DET process could, in principle, also be modulated by the orientation adopted by the phthalimide ring with respect to the peptide chain. Although the activation energy and the elongation of the scissile bond at the TS are similar for Φ_{hel} and Φ_{pII}, the latter conformer exhibits a larger electronic coupling between the D^- and A^- states. However, the computed rate constant for Φ_{pII} agrees less with the experimental results than that for Φ_{hel}. Furthermore, for Aib0, Φ_{hel} is more stable than Φ_{pII}, and thus Φ_{hel} should be the conformer more relevant for the DET.

4. Solvent has a significant effect on the shape of the PES, and the curve built in the gas phase shows anomalous features, mostly regarding the energy of the first excited state in the TS region and thus the computed energy gap. If solvent effects are not taken into account, the stability of a negative charge located on the relatively small peroxo moiety is considerably underestimated, and the completion of the DET process is delayed. This behavior also affects the predicted minimum energy structure in the proximity of the saddle point, giving a result that differs sharply from that computed in DMF solution. The DET rate constants computed on the basis of the "gas-phase" PES are significantly overestimated with respect to the experimental one.

These results highlight the fact that the PES associated with charge transfer processes must be built by performing geometry optimizations in solution. In those phenomena, the formation of weak hydrogen bond interactions, eventually requiring some conformational rearrangement, can indeed noticeably affect the activation free energy. A balanced description of hydrogen bond (in solution) and steric interaction is thus necessary when locating the energy minima or the saddle points. In this respect, it has been shown that PCM is able to reproduce the conformational behavior of biological molecules in polar solution, allowing a balanced treatment of conformers either in the presence or absence of intramolecular hydrogen bonds.[22]

5. The comparison between the results obtained for the systems containing methyl and *tert*-butyl terminal groups[13] shows that the rate constant is significantly affected by the substituents on the peroxide group. This result is not surprising per se since it could be expected that the substitution of the bulky *t*-butyl group with a methyl can affect the BDE of the peroxide and the $\Delta G^{\ddagger}$ for the DET reaction. On the other hand, it suggests that one must be cautious in interpreting the kinetic results, either experimental or computational, on the basis of simplified structural models.

The results of the present study, aside from the special focus on Aib-mediated DET, suggest the practical possibility of a general and flexible computational strategy allowing a more systematic computation of ET rates for systems of biological and technological relevance.[13] Such new developments should increase the ability of computational studies to complement experiments in the design of chemical compounds with specific electrochemical features. In a more general sense, reliable computational strategies would be of great value for unbiased investigations of the different chemicophysical effects controlling ET reactions and for testing different theories. It will clearly be an important development if the parameters entering the models used to interpret ET kinetics (based on the Marcus theory)[10] can be obtained by reliable quantum mechanical calculations with known "confidence ranges", since experimental estimates of the key energy and coupling quantities can be quite involved and strongly dependent on the model used to analyze the experimental results. Having an independent computational basis for determining the kinetic parameters will permit a refined, objective assessment of the reliability of a given kinetic model in accounting for observed kinetic data.

Acknowledgment. The financial support of the Italian Ministry for University and Research (MIUR) and of Gaussian, Inc. are gratefully acknowledged. All the calculations were

performed on the "Campus Grid" advanced computing facilities at the Università di Napoli "Federico II". M.D.N. was supported by the Division of Chemical Sciences, U.S. Department of Energy, under grant DE-AC02-98CH10886.

Supporting Information Available: Atomic numbers and Cartesian coordinates of the absolute minimum of Φ_{hel}Aib0 in the gas phase and of the g^-g^- and tg^- conformers of Φ_{hel}Aib0 and the absolute minimum of Φ_{pII}Aib0 in DMF solution, as well as a schematic drawing of the molecular orbital bearing the unpaired electron in the D^- state. This material is available free of charge via the Internet at http://pubs.acs.org.

References and Notes

(1) (a) *Organic Electrochemistry*; Lund, H., Baizer, M. M., Eds.; Dekker: New York, 1990. (b) Andrieux, C. P.; Saveant, J.-M. Electrochemical Reactions. In *Investigations of Rates and Mechanisms of Reactions*; Bernasconi, C. F. Ed.; Wiley and Sons: New York, 1986; Vol. 6, 4/E, Part 2C, p 305.

(2) Turner, A. P. F.; Karube, I.; Wilson, G. *Biosensors: Fundamentals and Applications*; Oxford University Press: New York, 1987.

(3) (a) *Molecular Electronics: Science and Technology*; Aviram, A., Ratner, M., Eds.; New York Academy of Sciences: New York, 1988. (b) Joachim, C.; Gimzewski, J. K.; Aviran, A. *Nature* **2000**, *408*, 541. (c) Fox, M. A. *Acc. Chem. Res.* **1999**, *32*, 201.

(4) (a) Marcus, R. A.; Sutin, N. *Biochim. Biophys. Acta* **1985**, *811*, 265. (b) Regan, J. J.; Onuchic, J. N. In *Electron Transfer: From Isolated Molecules to Biomolecules*; Jortner, J., Bixon, M., Eds.; Wiley: New York, 1999; Part 2, p 497.

(5) (a) Isied, S. S.; Ogawa, M. Y.; Wishart, J. F. *Chem. Rev.* **1992**, *92*, 381. (b) Mishra, A. K.; Chandrasekhar, R.; Faraggi, M.; Klapper, M. H. *J. Am. Chem. Soc.* **1994**, *116*, 1414. (c) Tamiaki, H.; Nomura, K.; Maruyama, K. *Bull. Chem. Soc. Jpn.* **1994**, *67*, 1863. (d) Bobrowski, K.; Holcman, J.; Poznanski, J.; Wierzchowski, K. L. *Biophys. Chem.* **1997**, *63*, 153. (e) Galka, M. M.; Kraatz, H.-B. *ChemPhysChem* **2002**, *3*, 356.

(6) (a) Antonello, S.; Formaggio, F.; Moretto, A.; Toniolo, C.; Maran, F. *J. Am. Chem. Soc.* **2003**, *125*, 2874. (b) Improta, R.; Antonello, S.; Formaggio, F.; Maran, F.; Rega, N.; Barone, V. *J. Phys. Chem. B* **2005**, *109*, 1023.

(7) (a) Burns, C. S.; Rochelle, L.; Forbes, M. D. *Org. Lett.* **2001**, *3*, 2197. (b) Sasaki, H.; Makino, M.; Sisido, M.; Smith, T. A.; Ghiggino, K. P. *J. Phys. Chem. B* **2001**, *105*, 10407. (c) Kise, K. J., Jr.; Bowler, B. E. *Inorg. Chem.* **2003**, *42*, 3891. (d) Morita, T.; Kimura, S. *J. Am. Chem. Soc.* **2003**, *125*, 8732.

(8) Maran, F.; Wayner, D. D. M.; Workentin, M. S. *Adv. Phys. Org. Chem.* **2001**, *36*, 85.

(9) (a) Antonello, S.; Musumeci, M.; Wayner, D. D. M.; Maran, F. *J. Am. Chem. Soc.* **1997**, *119*, 9541. (b) Antonello, S.; Maran, F. *J. Am. Chem. Soc.* **1999**, *121*, 9668. (c) Antonello, S.; Formaggio, F.; Moretto, A.; Toniolo, C.; Maran, F. *J. Am. Chem. Soc.* **2001**, *123*, 9577.

(10) (a) Newton, M. D. *Coord. Chem. Rev.* **2003**, *238*, 167. (b) Burghardt, I.; Laage, D.; Hynes, J. T. *J. Phys. Chem. A* **2003**, *107*, 11292. (c) Laage, D.; Burghardt, I.; Sommerfield, T.; Hynes, J. T. *ChemPhysChem* **2003**, *4*, 61. (d) Costentin, C.; Robert, M.; Saveant, J.-M. *J. Am. Chem. Soc.* **2004**, *126*, 16834. (e) Leontyev, I. V.; Basilevsky, M. V.; Newton, M. D. *Theor. Chem. Acc.* **2004**, *111*, 110. (f) Prytkova, T. R.; Kurnikov, I. V.; Beratan, D. N. *J. Phys. Chem. B* **2005**, *109*, 1618.

(11) (a) Saveant, J.-M. *J. Am. Chem. Soc.* **1987**, *109*, 6788. (b) Antonello, S.; Crisma, M.; Formaggio, F.; Moretto, A.; Taddei, F.; Toniolo, C.; Maran, F. *J. Am. Chem. Soc.* **2002**, *124*, 11503.

(12) German, E. D.; Kutznetov, A. M. *J. Phys. Chem.* **1994**, *98*, 6120.

(13) Improta, R.; Barone, V.; Newton, M. D. *ChemPhysChem*, in press.

(14) (a) Marcus, R. A. *J. Chem. Phys.* **1956**, *24*, 4966. (b) Hush, N. S. *J. Chem. Phys.* **1958**, *28*, 962. (c) Marcus, R. A. *Faraday Discuss. Chem. Soc.* **1982**, *74*, 7. (d) Saveant, J.-M. Single Electron Transfer and Nucleophilic Substitution. In *Advances in Physical Organic Chemistry*; Tidwell, T. T., Ed.; Academic Press: New York, 2000; Vol. 35, p 117.

(15) Frisch, M. J.; Trucks, G. W.; Schlegel, H. B.; Scuseria, G. E.; Robb, M. A.; Cheeseman, J. R.; Montgomery, Jr., J. A.; Vreven, T.; Kudin, K. N.; Burant, J. C.; Millam, J. M.; Iyengar, S. S.; Tomasi, J.; Barone, V.; Mennucci, B.; Cossi, M.; Scalmani, G.; Rega, N.; Petersson, G. A.; Nakatsuji, H.; Hada, M.; Ehara, M.; Toyota, K.; Fukuda, R.; Hasegawa, J.; Ishida, M.; Nakajima, T.; Honda, Y.; Kitao, O.; Nakai, H.; Klene, M.; Li, X.; Knox, J. E.; Hratchian, H. P.; Cross, J. B.; Bakken, V.; Adamo, C.; Jaramillo, J.; Gomperts, R.; Stratmann, R. E.; Yazyev, O.; Austin, A. J.; Cammi, R.; Pomelli, C.; Ochterski, J. W.; Ayala, P. Y.; Morokuma, K.; Voth, G. A.; Salvador, P.; Dannenberg, J. J.; Zakrzewski, V. G.; Dapprich, S.; Daniels, A. D.; Strain, M. C.; Farkas, O.; Malick, D. K.; Rabuck, A. D.; Raghavachari, K.; Foresman, J. B.; Ortiz, J. V.; Cui, Q.; Baboul, A. G.; Clifford, S.; Cioslowski, J.; Stefanov, B. B.; Liu, G.; Liashenko, A.; Piskorz, P.; Komaromi, I.; Martin, R. L.; Fox, D. J.; Keith, T.; Al-Laham, M. A.; Peng, C. Y.; Nanayakkara, A.; Challacombe, M.; Gill, P. M. W.; Johnson, B.; Chen, W.; Wong, M. W.; Gonzalez, C.; Pople, J. A. *Gaussian 03 Development Version*; revision D.02; Gaussian Inc.: Pittsburgh, PA, 2005.

(16) Adamo, C.; Cossi, M.; Barone, V. *J. Mol. Struct. (THEOCHEM)* **1999**, *493*, 145.

(17) Frisch, M. J.; Pople, J. A.; Binkley, J. S. *J. Chem. Phys.* **1984**, *80*, 3265.

(18) (a) Improta, R.; Barone, V. *J. Am. Chem. Soc.* **2004**, *126*, 14320. (b) Adamo, C.; Scuseria, G. E.; Barone, V. *J. Chem. Phys.* **1999**, *111*, 2889. (c) Cossi, M.; Barone, V. *J. Phys. Chem. A* **2000**, *104*, 10614. (d) Cossi, M.; Barone, V. *J. Chem. Phys.* **2001**, *115*, 4708. (e) Improta, R.; Santoro, F.; Dietl, C.; Papastathopoulos, E.; Gerber, G. *Chem. Phys. Lett.* **2004**, *387*, 509. (f) Aquilante, F.; Barone, V.; Roos, B. O. *J. Chem. Phys.* **2003**, *119*, 12323.

(19) Gawronski, J.; Kazmierczak, F.; Gawronska, K.; Rychlewska, U.; Norden, B.; Holmen, A. *J. Am. Chem. Soc.* **1998**, *120*, 12083.

(20) Cossi, M.; Scalmani, G.; Rega, N.; Barone, V. *J. Chem. Phys.* **2002**, *117*, 43.

(21) Miertus, S.; Scrocco, E.; Tomasi, J. *Chem. Phys.* **1981**, *55*, 117.

(22) Improta, R.; Barone, V. *Chem. Rev.* **2004**, *104*, 1231.

(23) (a) Cossi, M.; Barone, V. *J. Chem. Phys.* **2000**, *112*, 2427. (b) Cossi, M.; Barone, V. *J. Chem. Phys.* **2001**, *115*, 4708.

(24) Cave, R. J.; Newton, M. D. *Chem. Phys. Lett.* **1996**, *249*, 15.

(25) Antonello, S.; Crisma, M.; Formaggio, F.; Moretto, A.; Taddei, F.; Toniolo, C.; Maran, F. *J. Am. Chem. Soc.* **2002**, *124*, 11503.

(26) Donkers, R. L.; Maran, F.; Wayner, D. D. M.; Workentin, M. S. *J. Am. Chem. Soc.* **1999**, *121*, 7239.

(27) Maran, F.; Antonello, S. Università di Padova. Personal communication, 2005.